

Supplementary Materials for
Plagioclase under compression: A path to diaplectic glass and maskelynite

Tianqi Xie *et al.*

Corresponding author: Tianqi Xie, t.xie@usask.ca; Sean R. Shieh, sshieh@uwo.ca

Sci. Adv. **11**, eadv8231 (2025)
DOI: 10.1126/sciadv.adv8231

This PDF file includes:

Figs. S1 and S2
Tables S1 and S2
References

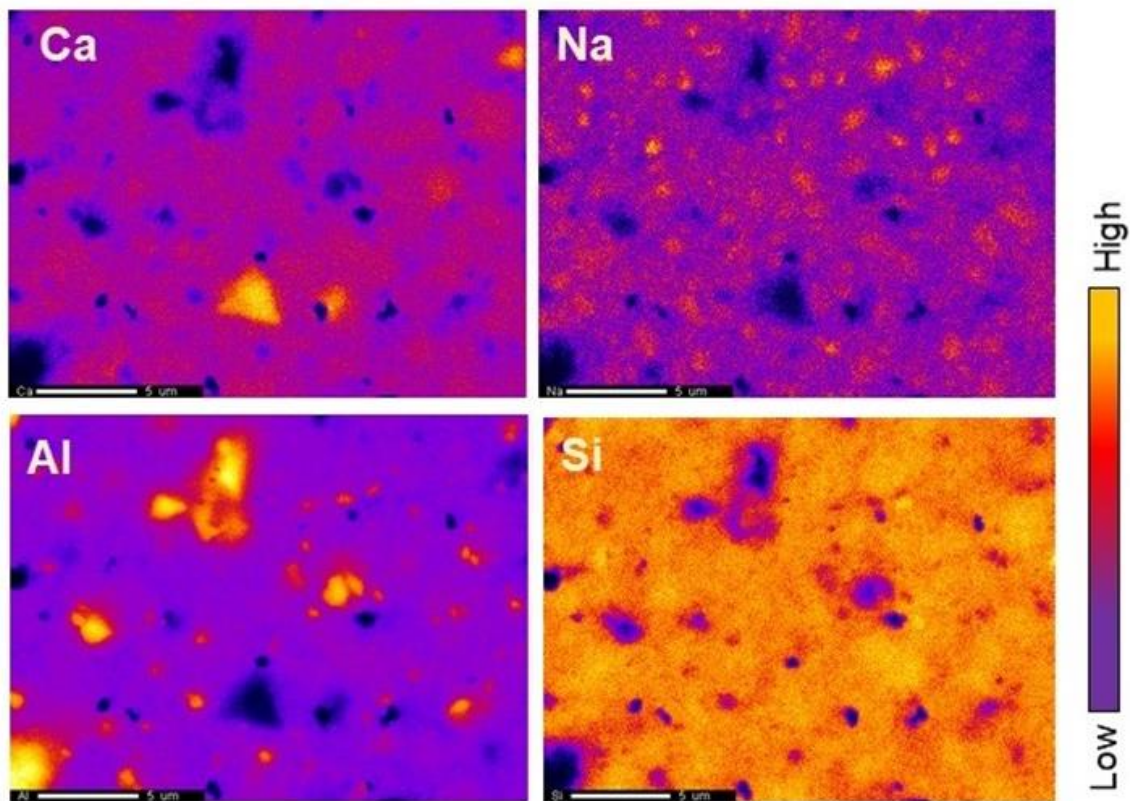


Figure S1. Element distribution of a heating spot. Element mapping of one heating spot (20 x 20 μm) associated with the quenched sample at 1 bar in Fig 1. From top to bottom shows the enrichment of calcium (Ca), sodium (Na), aluminium (Al), and silicon (Si); color scale bar on the right shows concentrations. The scale bar is 5 μm.

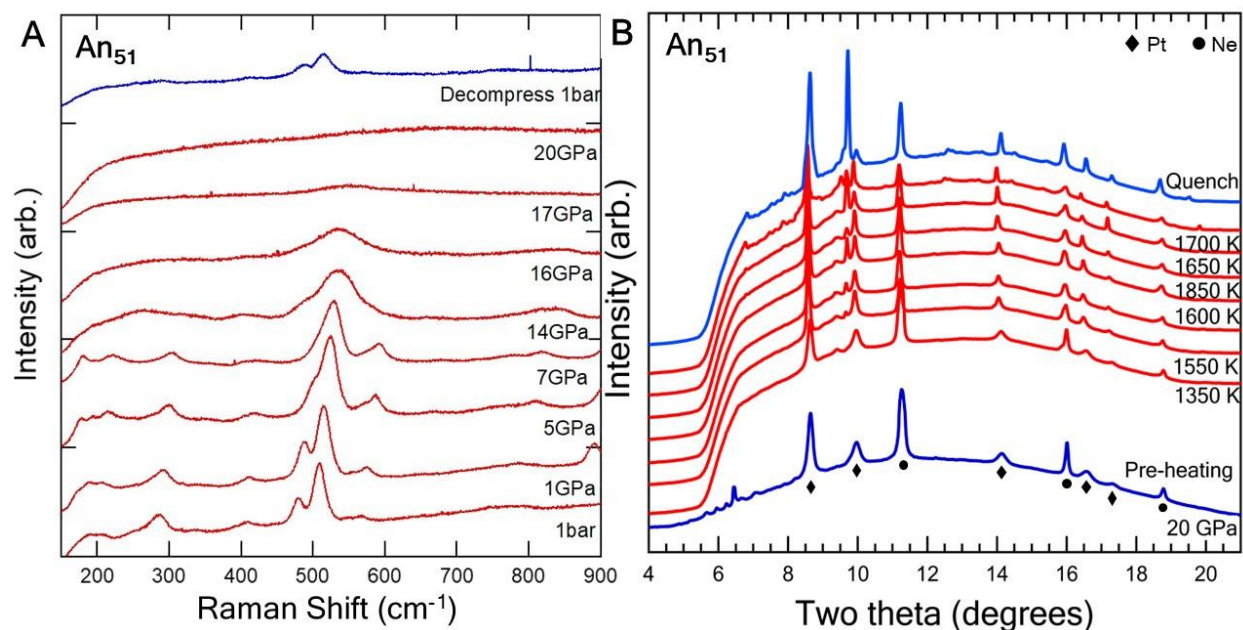


Figure S2. Amorphization of labradorite. (A) Raman spectra collected from labradorite An_{51} at 1 bar - 20 GPa and room temperature, showing the disappearance of the characteristic doublet peaks around 500 cm^{-1} , $\nu_s(\text{T-O-T})$ (symmetric T-O-T stretching) modes (T= Si or Al) (54) and the process of amorphization. The top spectrum was collected after decompression to 1 bar, and the main doublet feature was observed. This suggests part of the SiO_4 framework structure can be retained after decompression. (B) Synchrotron X-ray diffraction pattern collected from the heating circle at 19 GPa and temperatures from 1350 to 1700K, together with the quenched pattern after heating. In the pre-heating pattern at 20 GPa, the peaks below 8 degrees are from partially amorphous labradorite An_{51} . As temperature increases, disappearance of these peaks suggests the complete amorphization of labradorite. Pt: platinum, pressure marker, Ne: neon, pressure medium.

Table S1. Chemical composition of intermediate plagioclase labradorite An₅₁ and anorthite An₉₆ obtained by EPMA. wt% = mean composition in weight%; An-Ab-Or content in mol%.

Location	Labradorite	Anorthite
	Labrador, Canada	Miyake-Jima, Tokyo, Japan
	wt%	wt%
SiO ₂	56.23	44.57
Al ₂ O ₃	27.99	35.49
Na ₂ O	5.25	0.45
CaO	10.47	19.15
K ₂ O	0.39	0.02
FeO	0.23	0.39
MgO	0.01	0.09
TiO ₂	0.01	0.01
BaO	0.02	0.00
Total	100.58	100.17
An	51.25	95.83
Ab	46.48	4.08
Or	2.26	0.09

Table S2. Composition, crystal structure, bulk modulus and its pressure derivative for all phases observed in this study.

Phase	Composition	Crystal structure	Space group	K ₀ (GPa)	K' ₀	Reference
Au	Gold	Cubic	<i>Fm</i> $\bar{3}$ <i>m</i>	167	5.77(2)	(59)
Pt	Platinum	Cubic	<i>Fm</i> $\bar{3}$ <i>m</i>	277	4.95(2)	(59)
Jadeite	NaAlSi ₂ O ₆	Monoclinic	<i>C12/c1</i>	125.0	5.0	(64)
Stishovite	SiO ₂	Tetragonal	<i>P4</i> ₂ / <i>mn</i> <i>m</i>	304	4.6(1)	(65)
CaCl ₂ -type SiO ₂	SiO ₂	Orthorhombic	<i>Pnnm</i>	302	5.24(9)	(50)
CAS	CaAl ₄ Si ₂ O ₁₁	Hexagonal	<i>P6</i> ₃ / <i>mmc</i>	171	5.1	(66, 67)
Ca-Perovskite	CaSiO ₃	Cubic	<i>Pm</i> $\bar{3}$ <i>m</i>	223(6)	4.0	(68)
Corundum	Al ₂ O ₃	Hexagonal	<i>R</i> $\bar{3}$ <i>c</i>	252.9	4.251	(69)
Grossular	Ca ₃ Al ₂ Si ₃ O ₁₂	Cubic	<i>Ia</i> $\bar{3}$ <i>d</i>	166.5	4.96	(70)
CF	NaAlSiO ₄	Orthorhombic	<i>Pbnm</i>	220	4.1	(71)

REFERENCES AND NOTES

1. L. D. Ashwal, G. M. Bybee, Crustal evolution and the temporality of anorthosites. *Earth Sci. Rev.* **173**, 307–330 (2017).
2. L. D. Ashwal, Anorthosites, R. Asha, Ed. (Springer, Berlin, 1993).
3. W. L. Brown, I. Parsons, in *Feldspars and their Reactions*, I. Parsons, Ed. (Springer, 1994).
4. G. L. Hashimoto, M. Roos-Serote, S. Sugita, M. S. Gilmore, L. W. Kamp, R. W. Carlson, K. H. Baines, Felsic highland crust on Venus suggested by Galileo near-infrared mapping spectrometer data. *J. Geophys. Res.* **113**, E00B24 (2008).
5. B. Mason, Feldspar in chondrites. *Science* **148**, 943 (1965).
6. K. A. Milam, H. Y. McSween, J. Moersch, P. R. Christensen, Distribution and variation of plagioclase compositions on Mars. *J. Geophys. Res. Planets* **115**, 1–15 (2010).
7. A. L. Sprague, D. B. Nash, F. C. Witteborn, D. P. Cruikshank, Mercury's feldspar connection mid-IR measurements suggest plagioclase. *Adv. Space Res.* **19**, 1507–1510 (1997).
8. P. Gillet, A. El Goresy, Shock events in the solar system: The message from minerals in terrestrial planets and asteroids. *Annu. Rev. Earth Planet. Sci.* **41**, 257–285 (2013).
9. B. M. French, *Traces of catastrophe, a handbook of shock-metamorphic effects in terrestrial meteorite impact structures* (Lunar and Planetary Institute Houston, TX, 1998).
10. R. A. F. Grieve, G. R. Osinski, L. L. Tornabene, Planetary impacts, in *Encyclopedia of the Solar System* (Elsevier Inc., 2014).
11. A. E. Rubin, Maskelynite in asteroidal, lunar and planetary basaltic meteorites: An indicator of shock pressure during impact ejection from their parent bodies. *Icarus* **257**, 221–229 (2015).

12. D. Stöffler, C. Hamann, K. Metzler, Shock metamorphism of planetary silicate rocks and sediments: Proposal for an updated classification system. *Meteorit. Planet. Sci.* **53**, 5–49 (2018).
13. W. von Engelhardt, J. Arndt, D. Stöffler, W. F. Müller, H. Jeziorkowski, R. A. Gubser, Diaplektische Glaser in den Breccien des Ries von Nordlingen als Anzeichen für Stosswellenmetamorphose. *Contrib. Mineral. Petrol.* **15**, 93–102 (1967) [Diaplectic glasses in the breccias of the Nordlingen Ries as evidence of shock-wave metamorphism].
14. W. von Engelhardt, D. Stöffler, “Stages of shock metamorphism in crystalline rocks of the Ries basin, Germany,” in *Shock Metamorphism of Natural Materials*, B. M. French, N. M. Short, Eds. (Mono Book Corp., 1968), pp. 159–168.
15. P. B. Robertson, R. A. F. Grieve, Impact structures in Canada—Their recognition and characteristics. *J. Roy. Astron. Soc. Can.* **69**, 1–21 (1975).
16. T. Xie, G. R. Osinski, S. R. Shieh, Raman study of shock features in plagioclase feldspar from the Mistastin Lake impact structure, Canada. *Meteorit. Planet. Sci.* **55**, 1471–1490 (2020).
17. W. von Engelhardt, J. Arndt, W. F. Müller, D. Stöffler, Shock metamorphism in lunar samples. *Science* **167**, 669–670 (1970).
18. N. M. Short, The nature of the Moon’s surface: Evidence from shock metamorphism in Apollo 11 and 12 samples. *Icarus* **13**, 383–413 (1970).
19. S. J. Jaret, J. R. Johnson, M. Sims, N. DiFrancesco, T. D. Glotch, Micro spectroscopic and petrographic comparison of experimentally shocked albite, andesine, and bytownite. *J. Geophys. Res. Planets* **123**, 1701–1722 (2018).
20. J. Fritz, V. Assis Fernandes, A. Greshake, A. Holzwarth, U. Böttger, On the formation of diaplectic glass: Shock and thermal experiments with plagioclase of different chemical compositions. *Meteorit. Planet. Sci.* **54**, 1533–1547 (2019).

21. J. Hu, P. D. Asimow, Y. Liu, C. Ma, Shock-recovered maskelynite indicates low-pressure ejection of shergottites from Mars. *Sci. Adv.* **9**, eadf2906 (2023).
22. T. J. Ahrens, C. F. Petersen, J. T. Rosenberg, Shock compression of feldspars. *J. Geophys. Res.* **74**, 2727–2746 (1969).
23. R. V. Gibbons, T. J. Ahrens, Effects of shock pressures on calcic plagioclase. *Phys. Chem. Miner.* **1**, 95–107 (1977).
24. R. Jeanloz, T. J. Ahrens, Anorthite: Thermal equation of state to high pressures. *Geophys. J. Int.* **62**, 529–549 (1980).
25. R. Ostertag, Shock experiments on feldspar crystals. *J. Geophys. Res. Solid Earth* **88**, B364–B376 (1983).
26. D. J. Milton, P. S. De Carli, Maskelynite: Formation by explosive shock. *Science* **140**, 670–671 (1963).
27. Q. Williams, R. Jeanloz, Static amorphization of anorthite at 300 K and comparison with diaplectic glass. *Nature* **338**, 413–415 (1989).
28. N. Tomioka, H. Kondo, A. Kunikata, T. Nagai, Pressure-induced amorphization of albitic plagioclase in an externally heated diamond anvil cell. *Geophys. Res. Lett.* **37**, L21301 (2010).
29. T. Kubo, M. Kimura, T. Kato, M. Nishi, A. Tominaga, T. Kikegawa, K. Funakoshi, Plagioclase breakdown as an indicator for shock conditions of meteorites. *Nat. Geosci.* **3**, 41–45 (2010).
30. M. Sims, S. J. Jaret, E. Carl, B. Rhymer, N. Schrodt, V. Mohrholz, J. Smith, Z. Konopkova, H.-P. Liermann, T. D. Glotch, L. Ehm, Pressure-induced amorphization in plagioclase feldspars: A time-resolved powder diffraction study during rapid compression. *Earth Planet. Sci. Lett.* **507**, 166–174 (2019).

31. G. Tschermak, Die Meteoriten von Shergotty and Gopalpur, in *Sitzungsbericht der Kaiserlichen Akademieder Wissenschaften* (Wien, K.-K. Hof- und Staatsdruckerei in Commission bei C. Gerold's Sohn; 1872), vol. 65, pp. 122–146 [The Shergotty and Gopalpur meteorites].
32. G. Tschermak, Beitrag zur Klassifikation der Meteoriten. *Sitzber. Akad. Wiss. Wien Math.-Naturwiss. Kl. Abt. I* **88**, 347–371 (1883) [Contribution to the classification of meteorites].
33. R. A. Binns, Stony Meteorites bearing Maskelynite. *Nature* **213**, 1111–1112 (1967).
34. M. Chen, A. El Goresy, The nature of maskelynite in shocked meteorites: Not diaplectic glass but a glass quenched from shock-induced dense melt at high pressures. *Earth Planet. Sci. Lett.* **179**, 489–502 (2000).
35. A. El Goresy, P. Gillet, M. Miyahara, E. Ohtani, S. Ozawa, P. Beck, G. Montagnac, Shock-induced deformation of Shergottites: Shock-pressures and perturbations of magmatic ages on Mars. *Geochim. Cosmochim. Acta* **101**, 233–262 (2013).
36. N. L. Bowen, The melting phenomena of the plagioclase feldspars. *Am. J. Sci.* **35**, 577–599 (1913).
37. T. J. Ahrens, J. D. O'Keefe, Shock melting and vaporization of lunar rocks and minerals. *Moon* **4**, 214–249 (1972).
38. D. R. Schmitt, T. J. Ahrens, Temperatures of shock-induced shear instabilities and their relationship to fusion curves. *Geophys. Res. Lett.* **10**, 1077–1080 (1983).
39. J. R. Goldsmith, The melting and breakdown reactions of anorthite at high pressures and temperatures. *Am. Mineral.* **65**, 272–284 (1980).
40. M. B. Boslough, T. J. Ahrens, A. C. Mitchell, Shock temperatures in anorthite glass. *Geophys. J. Int.* **84**, 475–489 (1986).
41. L.-G. Liu, High-pressure phase transformations of albite, jadeite and nepheline. *Earth Planet. Sci. Lett.* **37**, 438–444 (1978).

42. D. C. Presnall, Phase diagrams of earth-forming minerals, in *Mineral Physics and Crystallography: A Handbook of Physical Constants AGU Ref. Shelf*, T. J. Ahrens, Ed. (AGU, Washington, D.C., 1995), vol. 2, pp. 248–268.
43. X. Liu, Phase relations in the system KAlSi_3O_8 - $\text{NaAlSi}_3\text{O}_8$ at high pressure-high temperature conditions and their implication to the petrogenesis of lingunite. *Earth Planet. Sci. Lett.* **246**, 317–325 (2006).
44. R. J. Angel, Order-disorder and the high-pressure P1-I1 transition in anorthite. *Am. Mineral.* **77**, 923–929 (1992).
45. T. P. Hackwell, R. J. Angel, Reversed brackets for the $\text{P}\bar{\text{I}}=\text{I}\bar{\text{I}}$ transition in anorthite at high pressures and temperatures. *Am. Mineral.* **80**, 239–246 (1995).
46. X. Liu, H. Ohfuji, N. Nishiyama, Q. He, T. Sanehira, T. Irifune, High-*P* behavior of anorthite composition and some phase relations of the $\text{CaO-Al}_2\text{O}_3$ - SiO_2 system to the lower mantle of the Earth, and their geophysical implications. *J. Geophys. Res. Solid Earth* **117**, B09205 (2012).
47. A. Pakhomova, D. Simonova, I. Koemets, E. Koemets, G. Aprilis, M. Bykov, L. Gorelova, T. Fedotenko, V. Prakapenka, L. Dubrovinsky, Polymorphism of feldspars above 10 GPa. *Nat. Commun.* **11**, 2721 (2020).
48. T. Kubo, M. Kono, M. Imamura, T. Kato, S. Uehara, T. Kondo, Y. Higo, Y. Tange, T. Kikegawa, Formation of a metastable hollandite phase from amorphous plagioclase: A possible origin of lingunite in shocked chondritic meteorites. *Phys. Earth Planet. In.* **272**, 50–57 (2017).
49. S. Ono, T. Iizuka, T. Kikegawa, Compressibility of the calcium aluminosilicate, CAS, phase to 44 GPa. *Phys. Earth Planet. In.* **150**, 331–338 (2005).
50. K. Ishibashi, K. Hirose, N. Sata, Y. Ohishi, Dissociation of CAS phase in the uppermost lower mantle. *Phys. Chem. Miner.* **35**, 197–200 (2008).

51. R. A. Fischer, A. J. Campbell, B. A. Chidester, D. M. Reaman, E. C. Thompson, J. S. Pigott, V. B. Prakapenka, J. S. Smith, Equations of state and phase boundary for stishovite and CaCl₂-type SiO₂. *Am. Mineral.* **103**, 792–802 (2018).
52. I. Daniel, P. Gillet, P. F. McMillan, G. H. Wolf, M. A. Verhelst, High-pressure behavior of anorthite: Compression and amorphization. *J. Geophys. Res.* **102**, 10313–10325 (1997).
53. R. A. F. Grieve, L. J. Pesonen, The terrestrial impact cratering record. *Tectonophysics* **216**, 1–30 (1992).
54. J. Hu, T. G. Sharp, Formation, preservation and extinction of high-pressure minerals in meteorites: temperature effects in shock metamorphism and shock classification. *Prog Earth Planet Sci* **9**, 6 (2022).
55. J. Fritz, A. Greshake, D. Stöffler, Micro-Raman spectroscopy of plagioclase and maskelynite in Martian meteorites: evidence of progressive shock metamorphism. *Antarct. Meteorite Res.* **18**, 96–116 (2005).
56. S. K. Sharma, B. Simons, H. S. Yoder, Raman study of anorthite, calcium Tschermak's pyroxene, and gehlenite in crystalline and glassy states. *Am. Mineral.* **68**, 1113–1125 (1983).
57. N. Tomioka, M. Miyahara, High-pressure minerals in shocked meteorites. *Meteorit. Planet. Sci.* **52**, 2017–2039 (2017).
58. O. Tschauner, C. Ma, Discovering high-pressure and high-temperature minerals, in *Celebrating the International Year of Mineralogy*, L. Bindi, G. Cruciani, Eds. (Springer, 2023).
59. Y. Fei, A. Ricolleau, M. Frank, K. Mibe, G. Shen, V. Prakapenka, Toward an internally consistent pressure scale. *Proc. Natl. Acad. Sci. U.S.A.* **104**, 9182–9186 (2007).
60. G. J. Piermarini, S. Block, J. D. Barnett, R. A. Forman, Calibration of the pressure dependence of the R₁ ruby fluorescence line to 195 kbar. *J. Appl. Phys.* **46**, 2774–2780 (1975).

61. H. K. Mao, J. Xu, P. M. Bell, Calibration of the ruby pressure gauge to 800 kbar under quasi-hydrostatic conditions. *J. Geophys. Res. Solid Earth* **91**, 4673–4676 (1986).
62. V. B. Prakapenka, A. Kubo, A. Kuznetsov, A. Laskin, O. Shkurikhin, P. Dera, M. L. Rivers, S. R. Sutton, Advanced flat top laser heating system for high pressure research at GSECARS: Application to the melting behavior of germanium. *High Press. Res.* **28**, 225–235 (2008).
63. C. Prescher, V. B. Prakapenka, *DIOPTAS*: A program for reduction of two-dimensional X-ray diffraction data and data exploration. *High Press. Res.* **35**, 223–230 (2015).
64. M. Akaogi, A. Tanaka, M. Kobayashi, N. Fukushima, T. Suzuki, High-pressure transformations in NaAlSiO_4 and thermodynamic properties of jadeite, nepheline, and calcium ferrite-type phase. *Phys. Earth Planet. In.* **130**, 49–58 (2002).
65. S. R. Shieh, T. S. Duffy, B. Li, Strength and elasticity of SiO_2 across the stishovite- CaCl_2 -type structural phase boundary. *Phys. Rev. Lett.* **89**, 255507 (2002).
66. S. Zhai, E. Ito, Phase relations of $\text{CaAl}_4\text{Si}_2\text{O}_{11}$ at high-pressure and high-temperature with implications for subducted continental crust into the deep mantle. *Phys. Earth Planet. In.* **167**, 161–167 (2008).
67. M. Akaogi, M. Haraguchi, K. Nakanishi, H. Ajiro, H. Kojitani, High-pressure phase relations in the system $\text{CaAl}_4\text{Si}_2\text{O}_{11}$ - $\text{NaAl}_3\text{Si}_3\text{O}_{11}$ with implication for Na-rich CAS phase in shocked Martian meteorites. *Earth Planet. Sci. Lett.* **289**, 503–508 (2010).
68. H. Chen, S.-H. Shim, K. Leinenweber, V. Prakapenka, Y. Meng, C. Prescher, Crystal structure of CaSiO_3 perovskite at 28–62 GPa and 300 K under quasi-hydrostatic stress conditions. *Am. Mineral.* **103**, 462–468 (2018).
69. A. Dewaele, M. Torrent, Equation of state of $\alpha\text{-Al}_2\text{O}_3$. *Phys. Rev. B* **88**, 64107 (2013).
70. S. Milani, R. J. Angel, L. Scandolo, M. L. Mazzucchelli, T. B. Ballaran, S. Klemme, M. C. Domeneghetti, R. Miletich, K. S. Scheidl, M. Derzsi, K. Tokár, M. Prencipe, M. Alvaro, F. Nestola, Thermo-elastic behavior of grossular garnet at high-pressures and temperatures. *Am. Mineral.* **102**, 851–859 (2017).

71. L. S. Dubrovinsky, N. A. Dubrovinskaia, V. B. Prokopenko, T. Le Bihan, Equation of state and crystal structure of NaAlSiO_4 with calcium-ferrite type structure in the conditions of the lower mantle. *High Press. Res.* **22**, 495–499 (2002).